JOURNAL OF SOLID STATE CHEMISTRY 105, 19–26 (1993)

Synthesis, Crystal Structure, and Magnetic Susceptibility of $MLnLiTeO_6$ (M = Ca, Sr, Ba)

M. L. LÓPEZ, A. JEREZ, C. PICO,* R. SÁEZ-PUCHE, AND M. L. VEIGA

Departamento de Química Inorgánica I, Facultad de Ciencias Químicas, Universidad Complutense, 28040 Madrid, Spain

Received July 7, 1992; in revised form October 26, 1992; accepted October 28, 1992

The mixed oxides $MLnLiTeO_6$ (M = Ca, Sr and Ba) were obtained by solid state reaction at temperature of 1073 K. X-ray diffraction data have been used to refine the crystal structures of ordered perovskites $MLnLiTeO_6$. $CaLnLiTeO_6$ and $SrLnLiTeO_6$ are monoclinic, with space group $P2_1/n$; $BaLnLiTeO_6$ shows cubic symmetry, with space group $Fm3m$. In these $MLnLiTeO_6$ compounds the Li^+ and Te^{6+} formal cations are ordered in B sites and the remaining M^{2+} and Ln^{3+} cations are randomly distributed on the 12-coordinate A sites. Unit cell parameters for these oxides can be related to a_p, that is, the parameter of the simple cubic perovskite. Magnetic properties are also presented and discussed.

Introduction

It is well known that in $A_2(BB')O_6$ and $(AA')(BB')O_6$ perovskites type (*1*) an ordered distribution of two kinds of B and B' cations along (111) planes is most probable when a large difference in either charge or ionic radii exists (*2*).

All these mixed oxides adopt perovskite-like structures with an ordered, alternate arrangement of cations on the octahedral (B) sites. An ordered distribution in the (BB') sites was reported for the compounds $M_2(B^{II}B^{V})O_6$ perovskites with M = Ca, Sr, or Ba (*3–8*), and where $(B^{II}B^{V})$ = (MgMo), (MgTa), (MgRu), or (MgIr).

Following these ideas this paper reports the synthesis and crystal structure determination of the mixed oxides $MLnLiTeO_6$, through the ideal substitution of the pair $(B^{II}B^{V})$ by the $(B^{I}B^{VI})$ one. In A sites are located the same alkaline-earth divalent cations (Ca, Sr, Ba) and some trivalent ions (La, Pr, Nd). These latter paramagnetic ions are isolated in the structure and the magnetic susceptibility measurements confirm this assumption.

Experimental

The different samples of $MLnLiTeO_6$ (M = Ba, Sr and Ca) were prepared from the appropriate amounts of $M(NO_3)_2$, $LiNO_3$, Ln_2O_3 (Pr_6O_{11}), and H_6TeO_6 (all supplied by Merck, Germany). The reaction mixtures were heated at 723 K followed by a further thermal treatment at 1073 K in air for 12 hr.

Powder X-ray diffraction patterns were registered at a rate of 0.1° (2θ) min^{-1} by means of a Siemens Kristalloflex diffractometer powered by a D500 generator using Ni filtered Cu$K\alpha$. A 2θ-step size of 0.04° was used. Rietveld's profile analysis method (*9*) was employed to refine the X-ray diffraction data in the different compounds $MLnLiTeO_6$.

Electron diffraction and high resolution electron microscopy were performed using

* To whom correspondence should be addressed.

0022-4596/93 $5.00

a Jeol 2000 FX and a Jeol 4000 EX microscope, respectively. The magnetic susceptibility measurements were made using the Faraday method in the temperature range 4.2 to 300 K using a DSM5 pendule susceptometer. The maximum applied magnetic field was 15 kG with $\mathbf{H}$ $(d\mathbf{H}/dz)$ = 29 kG^2 cm^{-1}. The equipment was calibrated with $Hg(Co(SCN)_4)$ and $Gd_2(SO_4)_3 \cdot 8H_2O$; χ was independent of the field in the temperature range of measurements. Values of effective magnetic moment (μ_B) and Weiss constant (θ) were obtained by least-square fits from the linear part of the χ^{-1} vs T plots.

Results and Discussion

1. Structural Characterization

The solid single phases studied here are obtained as polycrystalline powders; the previous structural results indicate significant differences between the Ba*Ln*LiTeO$_6$ derivatives and the remaining calcium and strontium derivatives. The discussion is presented separately, starting with the former series, which possess the higher symmetry.

For Ba*Ln*LiTeO$_6$ (*Ln* = La, Pr, and Nd) X-ray diffraction data indicate that these mixed oxides have the characteristic reflections of a perovskite structure. The crystal parameters are listed in Table I, on the basis of a cubic unit cell. Rietveld's profile analysis method was applied for refinement of the $BaPrLiTeO_6$ from X-ray diffraction results. Refinements were carried out in the cubic space group *Fm*3*m*, with a unit cell of approximate size $2a_p$ (a_p is the parameter of the simple cubic perovskite structure).

TABLE I

CELL PARAMETERS OF Ba*Ln*LiTeO$_6$

Ln	*a*(Å)	*V*(Å^3)
La	8.036(2)	518.9
Pr	8.028(1)	517.5
Nd	8.026(2)	517.1

These data suggest an ordered arrangement of cations on the *B* sites (*3*), as it is shown in Fig. 1a. The model provides good agreement between observed and calculated X-ray diffraction profiles (Fig. 2). In this structure both Pr and Ba are the large cations occupying an anion position in a ccp arrangement, while Li and Te occupy the octahedral sites (corners in the ideal perovskite structure). Crystal data for these compounds are given in Table II on the basis of the space group *Fm*3*m*. The profile *R* factors R_p, R_{wp}, and R_B are indicative of a reliable structural model.

The bond distances are listed in Table III; they agree with the sums of the ionic radii

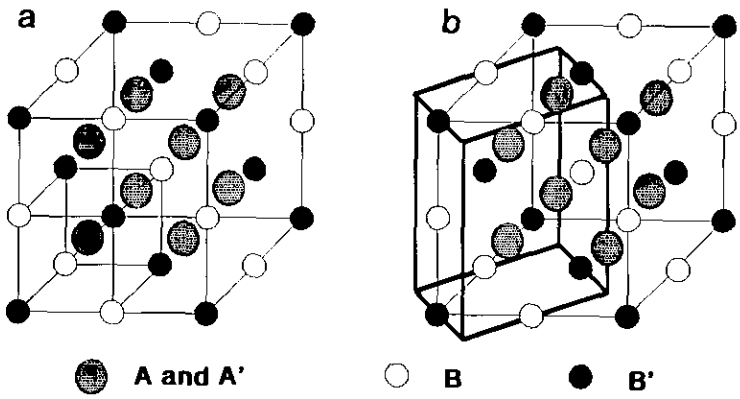

FIG. 1. Structural model of perovskites $AA'BB'O_6$. (a) Cubic: *Fm*3*m*, $a = 2a_p$. (b) Monoclinic: $a \approx b \approx \sqrt{2}\, a_p$, $c \approx 2a_p$.

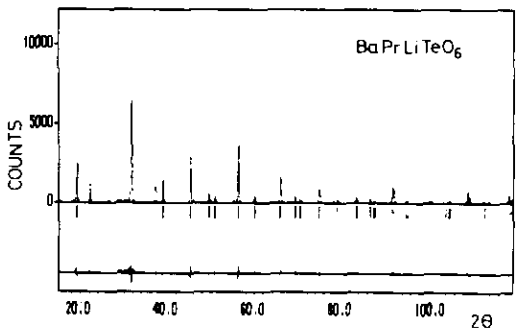

FIG. 2. The observed (. . .), calculated (—), and difference diffraction profiles for BaPrLiTeO$_6$.

as given by Shannon (*10*) (mean values in the case of Ba/Pr lengths).

The results of X-ray diffraction for BaLnLiTeO$_6$ (Ln = La and Nd) were similar to those for BaPrLiTeO$_6$ and the crystal structures therefore were refined in the same space group $Fm3m$, as described above. As an example, Fig. 3a shows an electron diffraction pattern along the [001] zone axis for BaNdLiTeO$_6$, which confirms the cubic symmetry of the material. The ordering is evident in two normal directions (interplanar distances of 8.0 Å), as is shown in the corresponding electron micrograph (Fig. 3b). From the identities of the different patterns obtained, we can conclude the presence of pure phases, as well as in the other materials which are discussed later.

TABLE II

REFINED STRUCTURAL PARAMETERS FOR BaPrLiTeO$_6$[a]

Atom	Site	x	y	z
Ba/Pr	8c	$\frac{1}{4}$	$\frac{1}{4}$	$\frac{1}{4}$
Li	4a	0	0	0
Te	4b	$\frac{1}{2}$	$\frac{1}{2}$	$\frac{1}{2}$
O	24e	0.2545(2)	0	0

[a] Cubic, $Fm3m$: a = 8.028(2) Å, R_B = 4.25, R_{wp} = 20.7, R_p = 14.5, χ^2 = 5.15.

TABLE III

BOND LENGTHS (IN Å) FOR BaPrLiTeO$_6$

Ba/Pr–O	2.838(2)	×12	2.83[a]
Li–O	2.043(2)	×6	2.14[a]
Te–O	1.971(7)	×6	1.96[a]

[a] Values from Shannon (*10*).

In $A_2(BB')O_6$ perovskites B and B' ions can be ordered in such a manner that each BO_6 octahedron links six $B'O_6$ and vice versa. When the A cations are slightly too small for adopt a cubooctahedral coordination, the ReO_3-like framework collapses (reducing some A–O bond lengths and therefore its coordination number) by a correlated tilting of the BO_6 and $B'O_6$ octahedra in their corner-connected array.

On the other hand, the X-ray diffraction patterns of CaPrLiTeO$_6$ and SrPrLiTeO$_6$ were indexed by a monoclinic unit cell. The agreement between the observed and calculated profiles is shown in Fig. 4. These compounds were refined in space group $P2_1/n$, which also permits an ordered arrangement of B-sites but in a unit cell of size $\sqrt{2}\ a_p \times \sqrt{2}\ a_p \times 2\ a_p$ (see Fig. 1b). The refined structural parameters are listed in Tables IV and V.

The most representative bond lengths are given in Tables VI and VII for both com-

TABLE IV

STRUCTURAL PARAMETERS FOR CaPrLiTeO$_6$[a]

Atom	Site	x	y	z
Ca/Pr	4e	0.508(7)	0.548(3)	0.249(4)
Li	2d	$\frac{1}{2}$	0	0
Te	2c	0	$\frac{1}{2}$	0
O1	4e	0.192(3)	0.213(3)	−0.045(2)
O2	4e	0.291(3)	0.694(3)	−0.034(3)
O3	4e	0.399(3)	0.971(2)	0.255(2)

[a] Monoclinic, $P2_1/n$: a = 5.512(2), b = 5.646(2), c = 7.806(2) Å, β = 90.04(3)°, R_B = 4.85, R_{wp} = 17.7, R_p = 16.8, χ^2 = 1.93.

TABLE V

STRUCTURAL PARAMETERS FOR $SrPrLiTeO_6$[a]

Atom	Site	x	y	z
Sr/Pr	4*e*	0.504(2)	0.526(5)	0.249(1)
Li	2*d*	½	0	0
Te	2*c*	0	½	0
O1	4*e*	0.266(1)	0.285(1)	0.048(8)
O2	4*e*	0.331(1)	0.721(9)	0.010(8)
O3	4*e*	0.429(1)	0.988(5)	0.281(6)

[a] Monoclinic, $P2_1/n$: a = 5.598(7), b = 5.594(6), c = 7.929(7) Å, β = 90.04(3)°, R_B = 6.01, R_{wp} = 18.7, R_p = 20.3, χ^2 = 2.43.

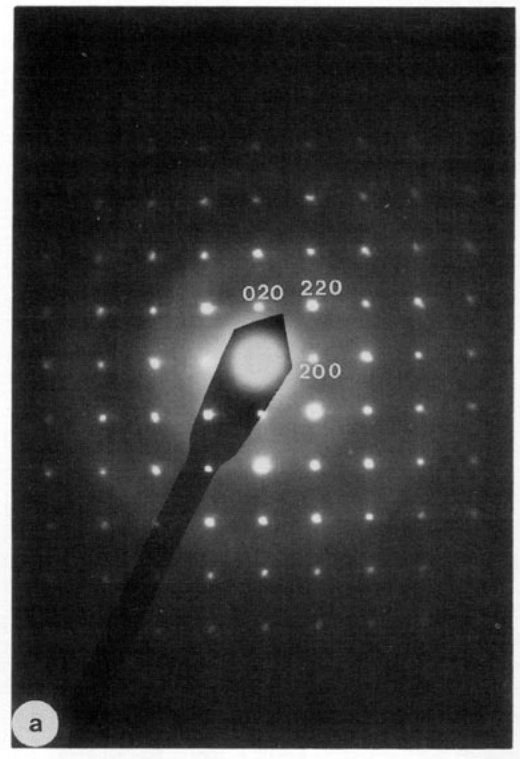

FIG. 3. (a) Electron diffraction pattern (Jeol 4000Ex) along [001] zone axis for $BaNdLiTeO_6$; (b) the corresponding electron micrograph.

pounds. Due to the lower scattering power of oxygen and lithium atoms, the values for metal–oxygen bond distances are not very reliable in these cases.

All members of the system $MLnLiTeO_6$ (M = Ca and Sr) described here are isostructural and the resulting lattice parameters (also obtained by Rietveld's method), are gathered in Table VIII.

In Megaw's analysis (*11*) for the $GdFeO_3$ two independent rotation angles are used, $j(B)$ about [110] and $w(B)$ about [001] of the perovskite prototype. The formulae obtained by Groen *et al.* (*12*) are used. The parameters w and j for BO_6 and $B'O_6$ can be derived in two ways: (1) From the lattice parameters (a, b, c) and the B–O and the B'–O distances calculated from the Shannon radii (assuming regular octahedra); and (2) from the atomic positions without any assumptions at all. The tilt angles for the $CaLnLiTeO_6$ and $SrLnLiTeO_6$ have been calculated from the atomic coordinates. In

TABLE VI

BOND LENGTHS (IN Å) FOR $CaPrLiTeO_6$

Li–O1	2.106(1) × 2	Te–O1	1.970(9) × 2
Li–O2	2.091(2) × 2	Te–O2	1.963(1) × 2
Li–O3	2.078(1) × 2	Te–O3	1.992(5) × 2
Mean:	2.09	Mean:	1.97
Shannon:	2.14	Shannon:	1.96

Ca/Pr–O1	Ca/Pr–O2	Ca/Pr–O3
2.732(7)	2.643(5)	2.459(3)
2.398(2)	2.713(6)	2.293(6)
2.664(4)	2.436(6)	
	Mean: 2.54	
	Shannon: 2.52	

TABLE VII

BOND LENGTHS (IN Å) FOR $SrPrLiTeO_6$

Li–O1	2.207(1) × 2	Te–O1	1.899(9) × 2
Li–O2	1.990(2) × 2	Te–O2	1.992(1) × 2
Li–O3	1.892(1) × 2	Te–O3	2.119(5) × 2
Mean:	2.03	Mean:	2.00
Shannon:	2.14	Shannon:	1.96

Sr/Pr–O1	Sr/Pr–O2	Sr/Pr–O3
2.627(7)	2.782(5)	2.632(3)
2.350(2)	2.685(6)	2.515(6)
2.937(4)	2.702(6)	
	Mean: 2.65	
	Shannon: 2.59	

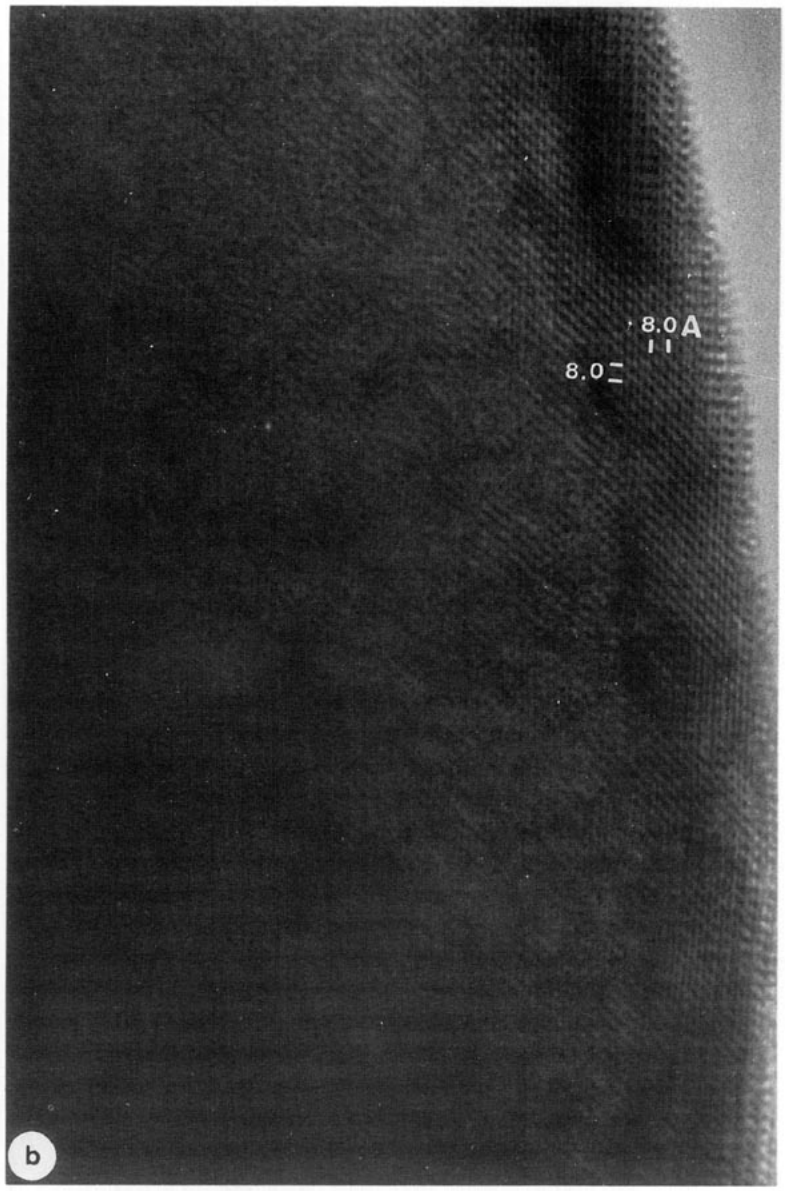

FIG. 3—*Continued*

Table IX the results obtained for the tilt angles are gathered. Although these compounds are pseudocubic, there exists a considerable rotation of the octahedra in the cubic prototype structure. This rotation determines the eight-coordination of Ln^{3+} and M^{2+} ions in the hole defined by the $B(B')O_6$ octahedra.

In the same manner, the electron diffraction patterns of $CaPrLiTeO_6$ suggest that this phase cannot be described by means of a cubic symmetry. Figure 5 gives the electron diffraction pattern along the zone axis [001], which is consistent with a monoclinic symmetry. The relation between the cubic ideal perovskite parameter and the monoclinic ones has been represented by the respective Miller indices.

TABLE VIII

CELL PARAMETERS OF MLnLiTeO$_6$ (M = Ca AND Sr)

Compound	a(Å)	b(Å)	c(Å)	β(°)	V(Å^3)
CaLaLiTeO$_6$	5.555(9)	5.612(9)	7.868(2)	90.03(3)	245.3
CaPrLiTeO$_6$	5.512(2)	5.646(2)	7.806(2)	90.3(3)	242.9
CaNdLiTeO$_6$	5.490(3)	5.647(1)	7.784(3)	90.4(1)	241.3
SrLaLiTeO$_6$	5.593(3)	5.629(3)	7.931(5)	90.05(1)	249.9
SrPrLiTeO$_6$	5.598(7)	5.594(6)	7.929(7)	90.1(1)	248.4
SrNdLiTeO$_6$	5.604(2)	5.592(1)	7.908(2)	90.1(3)	247.8
SrSmLiTeO$_6$	5.564(3)	5.640(3)	7.871(4)	90.1(6)	247.0
SrEuLiTeO$_6$	5.562(3)	5.643(3)	7.860(5)	90.1(8)	246.3
SrGdLiTeO$_6$	5.539(3)	5.660(3)	7.851(5)	90.2(5)	246.2

2. *Magnetic Properties*

The magnetic susceptibilities of CaPrLiTeO$_6$ and SrPrLiTeO$_6$ follow Curie–Weiss behavior from 300 to 30 K. Below this temperature, deviations upward from linearity are observed, analogous to those found in some compounds of praseodymium (*13*). Since this cation has an even number of f electrons, the lowest crystal field level could

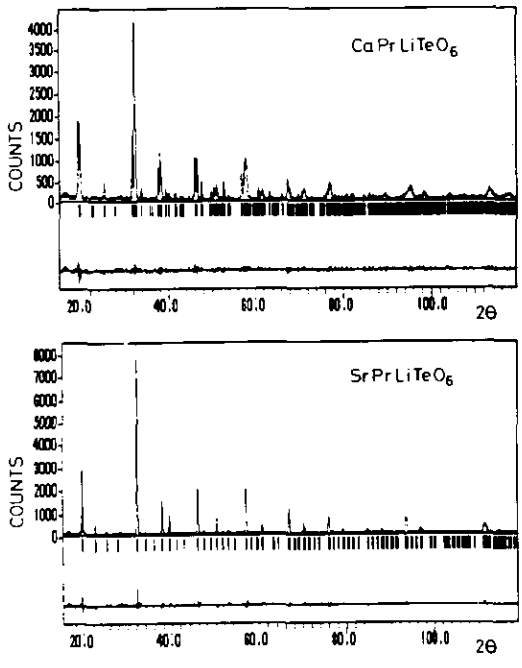

FIG. 4. The observed (. . .), calculated (—), and difference diffraction profiles for CaPrLiTeO$_6$ and SrPrLiTeO$_6$.

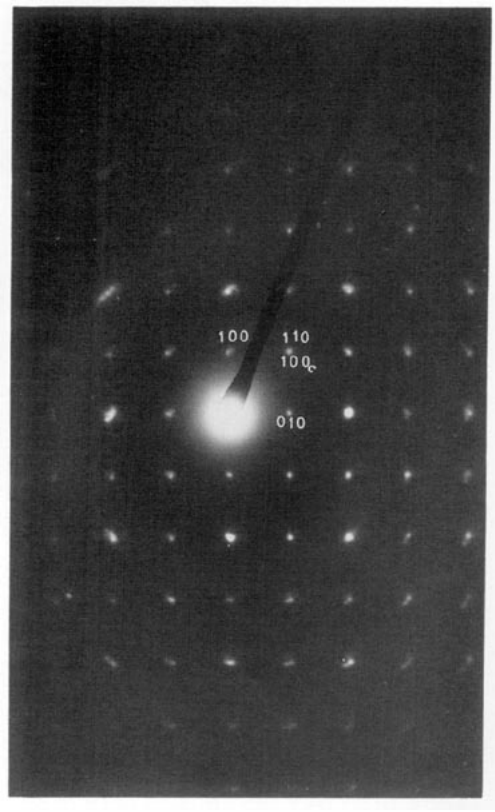

FIG. 5. Electron diffraction pattern (Jeol 2000Fx) along [001] zone axis for CaPrLiTeO$_6$.

TABLE IX

TILT ANGLES (°) FOR Li AND Te OCTAHEDRA IN CaLnLiTeO_6 AND SrLnLiTeO_6

Compound	w(Li)	w(Te)	j(Li)	j(Te)
CaLaLiTeO_6	8.8	8.4	14.9	14.2
CaPrLiTeO_6	11.2	10.5	16.2	16.8
CaNdLiTeO_6	9.3	8.8	15.8	15.7
SrLaLiTeO_6	3.2	4.2	2.7	2.7
SrPrLiTeO_6	3.9	2.9	10.2	13.2
SrSmLiTeO_6	9.1	9.5	12.3	12.1
SrEuLiTeO_6	11.2	10.4	13.1	12.9
SrGdLiTeO_6	10.1	9.9	12.9	13.1

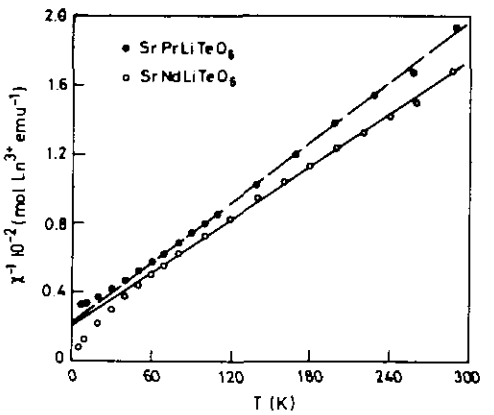

FIG. 7. Temperature dependence of the reciprocal molar susceptibility of SrPrLiTeO_6 and SrNdLiTeO_6.

be singlet and the upward deviations observed at the lower temperatures are probably due to the population of this singlet level (Figs. 6 and 7).

The reciprocal molar susceptibility for SrNdLiTeO_6 and BaNdLiTeO_6 obey a Curie–Weiss law, Figs. 7 and 8, above 40 K and the calculated magnetic moment from the χ^{-1} vs T plot agrees with the expected one for isolated Nd^{3+} ions in both compounds (see Table X). The temperature dependence of χ below 40 K, which appears to follow a second Curie–Weiss law, shows crystal field effects. Similar remarks have previously been reported for different neodymium compounds (*14*). The negative values for the Weiss constant obtained for all these compounds are entirely due to crystal field effects and noncooperative interactions; i.e., antiferromagnetic coupling is not operative in these compounds down to 4.2 K. Optical spectra experiments are now in progress in order to evaluate the crystal field parameters needed to simulate the obtained low temperature magnetic susceptibility data.

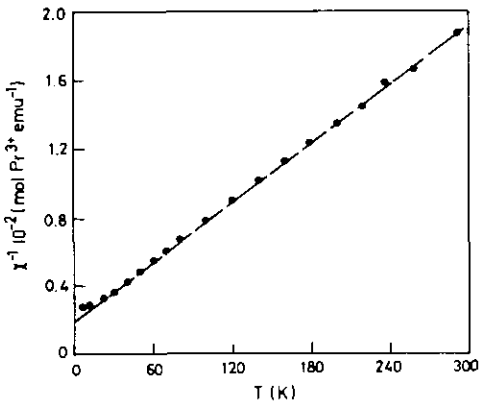

FIG. 6. Temperature dependence of the reciprocal molar susceptibility of CaPrLiTeO_6.

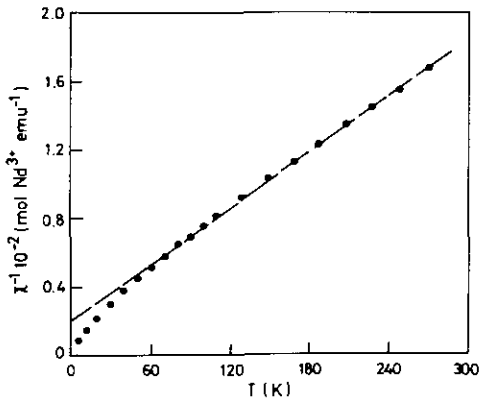

FIG. 8. Temperature dependence of the reciprocal molar susceptibility of BaNdLiTeO_6.

TABLE X

MAGNETIC PARAMETERS FOR MLnLiTeO$_6$ (M = Ca, Sr, AND Ba)

Compound	Ground state of the free ion	μ^C(B.M.)[a]	μ^E(B.M.)[b]	θ(K)
CaPrLiTeO$_6$	$^3H_4$	3.60	3.75	−36.7
SrPrLiTeO$_6$			3.77	−42.4
SrNdLiTeO$_6$	$^4I_{9/2}$	3.62	3.79	−20.9
BaNdLiTeO$_6$			3.81	−35.9

[a] Calculated magnetic moments.
[b] Experimental magnetic moments.

Acknowledgments

The authors are grateful for CICYT support (PB 89/134 and ID 90/725) and M. L. López is grateful to the Universidad Complutense de Madrid for the "Beca Complutense."

References

1. A. R. WEST, "Solid State Chemistry and its Applications," Wiley, Oxford (1990).
2. F. GALASSO AND J. PYLE, *Inorg. Chem.* **2,** 482 (1963).
3. J. H. CHOY, S. T. HONG, AND H. M. SUH, *Bull. Korean Chem. Soc.* **9,** 395 (1988).
4. M. WALEWSKI, B. BUFFAT, G. DEMAZEAU, F. WAGNER, M. POUCHARD, AND P. HAGENMULLER, *Mater. Res. Bull.* **18,** 881 (1973).
5. G. BLASSE, *J. Inorg. Nucl. Chem.* **27,** 993 (1965).
6. T. NAKAMURA AND J. H. CHOY, *J. Solid State Chem.* **20,** 233 (1977).
7. J. H. CHOY AND S. T. HONG, *Bull. Korean Chem. Soc.* **10,** 8 (1989).
8. I. FERNÁNDEZ, R. GRATREX, AND N. N. GREENWOOD, *J. Solid State Chem.* **32,** 97 (1980).
9. R. RODRÍGUEZ-CARVAJAL, "Fullprof" program, ILL Grenoble, France (1990).
10. R. B. SHANNON, *Acta Crystallogr. Sect. A* **32,** 751 (1976).
11. H. D. MEGAW, *J. Phys. (Paris)* **33** (C2), 1 (1972).
12. W. A. GROEN, F. P. F. VAN BERKEL, AND D. J. W. IJDO, *Acta Crystallogr. Sect. C* **42,** 1972 (1986).
13. R. SAEZ-PUCHE, M. NORTON, T. R. WHITE, AND W. S. GLAUSSINGER, *J. Solid State Chem.* **50,** 281 (1981).
14. M. L. LÓPEZ, M. L. VEIGA, F. FERNÁNDEZ, A. JEREZ, AND C. PICO, *J. Less-Common Met.* **166,** 367 (1990).